TWO-STEP-METHOD FOR THE CALCULATION OF WALL INTERFERENCES IN SLOTTED TEST SECTIONS

J. Amecke

Deutsche Forschungsanstalt für Luft- und Raumfahrt e.V.,
Göttingen, Germany

Abstract

For wind tunnel test sections with adjustable slotted walls and 2D-models a "Two-Step-Method" has been developed for the determination of the residual interferences and the effective contour of an virtual adaptive wall.

The method is based on two corresponding tests one with closed and one with open slots, and all other conditions unchanged. No model representation is required.

The method has been checked systematically in the Transonic Wind Tunnel Göttingen.

Nomenclature

$c_p = \frac{p - p_\infty}{\frac{\rho_\infty}{2} \cdot U_\infty^2}$	pressure coefficient
c_D	drag coefficient (eq. 20)
D	profile drag
h	test section height
L	profile chord length
Ma	Mach number
U	velocity component in x-direction
$u = \frac{U}{U_\infty} - 1$	dimensionless perturbation velocity in x-direction
V	velocity component in y-direction
$v = \frac{V}{U_\infty}$	dimensionless perturbation velocity in y-direction
W	test section width
x, y	field point within the test section
α	angle of incidence
$\beta = \sqrt{1 - Ma_\infty^2}$	Prandtl factor
γ	vortex distribution
ΔH	deflection of the test section height on account of adaptation
ρ	density
ξ, η	coordinates of a running point for the integration
σ	open-area ratio of the slotted wall

Upper subscripts:

i	wall-induced
m	model-induced

Lower subscripts:

c	measurement with closed walls
e	test section exit
i	test section inlet
l	lower test section wall
s	measurement with slotted walls
u	upper test section wall
∞	undisturbed flow field

1. Introduction

A body in an unlimited flow field causes disturbances, which are diminishing slowly with increasing distance from the body. This has consequences for the investigation of a model in a wind tunnel, because this flow field is limited by the test section walls. The so-called "wall interferences" may be neglected only,

- if the model is small in relation to the size of the test section or
- if the test section walls are shaped especially for the suppression of the wall interferences.

For subsonic wind tunnels mainly test sections with open or closed walls are in use. With respect to the wall interferences both types are not perfect, but of opposite effect [1].

In a closed test section the blockage of the model induces a positive interference velocity (i.e. the velocities in the wind tunnel are increased compared with free-flight conditions). Vice versa in an open test section the blockage of the model induces a negative interference velocity.

A lifting body effects an upwash in a closed test section (i.e. an increasing of the lift) and a downwash of the same value in an open test section.

Therefore it can be expected, that a partially open test section wall will cause only little or no interferences.

For the required openings in principal an infinity of arrangements is conceivable. But of practical importance are only walls with circular holes (perforation) or longitudinal slots. The following investigation is confined to the latter only.

In general the optimum opening of the slots is determined empirically. Therefore it is usual to perform test series with one or more models, from which the interference-free results are known. The slots have to be adjusted until the actual results are well in accordance with the interference-free results. These interference-free results can be obtained:

- by tests with the identical model in a considerable larger test section or
- by tests with a geometrical similar, but considerable smaller model in the same test section.

It is assumed, that the determined optimum slot opening is valid also for other model shapes or model positions.

It would be desirable to overcome this empirical procedure by a (theoretical based) method, which allows the definition of the optimum slot opening without comparative tests in another wind tunnel or with another model.

In the following a method for the evaluation of the wall interferences in test sections with longitudinal slotted walls is presented. One important feature of this method is, that it is based on the wall pressure distribution only and requires no model representation.

2. Wall Interferences in Test-Sections with Slotted Walls

For two-dimensional tests in the subsonic range test sections with two (opposite) slotted walls are well approved. They are fitted to compensate the wall interferences caused as well by the blockage as by the lift of a model.

For the valuation of the interaction between slots and wall interferences it is necessary to analyse the wall induced flow field. If furthermore the slot opening is adjustable, this opening may be changed until the interferences are a minimum.

The "classic" method for the calculation of the wall interferences is based on the small perturbation theory. The boundary conditions at the wall are defined as follows:

- The velocity component parallel to the wall vanishes in the slot plane;
  i.e. "Boundary condition of the **open** test section"
- The velocitiy component normal to the wall vanishes at the solid part of the wall;
  i.e. "Boundary conditon of the **closed** test section".

With the assumption of a large number of slots and by application of the slender body theory local at the wall, it is possible to reduce the mixed boundary condition into an equivalent homogeneous one with the same solution in the center of the test section [2], [3], [4], [5].

It turns out by a thorough analysis as presented by Berndt [6], that the referred method does not describe the flow field sufficient. The improvement of the classical method failed since today, because of the principle impossibility to calculate the viscous flow effects in the slot region.

Since the width of the slots is small compared with the width of the test section wall, it may be assumed that the distinct influence of a single slot diminishes fast with increasing distance from the slot. Consequently if the model is not too large, a zone between wall and model exists in which:

- the model-induced disturbances are diminished so far that the application of the small perturbation theory is admissible and
- the slot-induced disturbances are diminished so far, that the flow field may be treated as homogeneous.

On these premises it is possible to calculate the wall interferences at the location of the model from the velocity distribution on a closed line around the model [7]. But the practical execution of this calculation is hampered by the difficulty to acquire the test data. It turns out that both components of the velocity are required. But especially the acurate measurement of the normal component is very difficult, because it is extremly small related to the longitudinal component. One thorough investigated method is the tube probe ("Calspan Tube" [8]).

The measurement of two components at one line can be replaced by the measurement of one component at two lines. A test arrangement based on this method is described in [9]. It comprises a test section with side walls of glass and a movable Laser-Doppler-Anemometer outside.

Summarizing it has to be stated that all methods discussed above are not fully satisfying. The basic problem is that the slope of the streamlines close to the (straight) test section wall is extremely small. Presently no method is available to carry out the measurements with the required accuracy at all. The execution of this measurement under routine conditions during a wind tunnel test seems an unattainable goal.

3. Explanation of the Two-Step-Method

Subsequently a new approach is presented for the analysis of the effective wall contour resp. the residual interferences in a test section with slotted walls. It is the scope of this new method to overcome the deficiencies of the presently available methods.

This so-called "Two-Step-Method" is applicable for slotted test sections with adjustable slot open-area ratios between zero (closed) and about 10%.

For the application of this method an algorithm is required for the calculation of the wall induced flow field from the velocity distribution at the wall. In a small perturbation field the u-component is derived from the static pressure at the wall and the v-component from the slope of the wall.

The fundamental idea of the new method is to take two measurements for every test point under following stipulation:

1. Measurement of the wall pressure distribution with **closed slots.** From these values the complete description of the model-induced flow field is derived.
2. Measurement of the wall pressure distribution with ***open slots*** and all other parameters unchanged. During this measurement the model-induced flow field remains unchanged. The opening of the slots changes only the wall-induced flow field.

   Referring to the investigation of Firmin and Cook [10] it is assumed, that the pressure distribution in the center-line of the central slat represents correctly the u-component of the homogeneous flow and is not affected by the cross-flow induced by the slots.

From the result of both measurements the v-component of the homogeneous flow at the wall and consequently the wall shape can be evaluated.

In general the method can be applied to any wall shape as far as the linearized theory is valid. Nevertheless the following presentation is restricted to straight walls, because this case is especially of practical interest.

The analysis of the two partial tests takes place according to following procedure (Nomenclature see **Figure 1):**

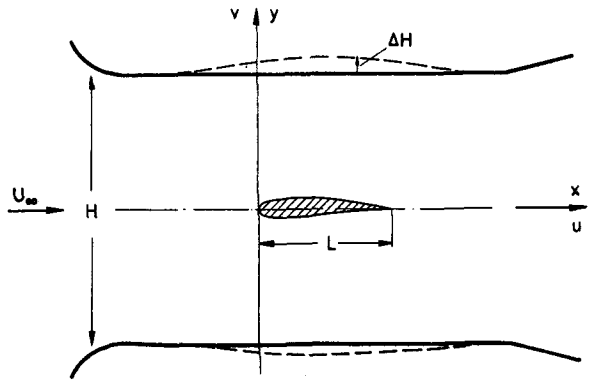

Figure 1. Nomenclature
Upper and lower wall closed resp. with longitudinal slots

1. Calculation of the wall velocities from the measured wall pressure distribution with closed slots:

$$u_c(x) = -\frac{(c_p)_c}{2}$$
$$v_c(x) \equiv 0 \text{ (straight wall!)}$$

2. Calculation of the wall induced interference velocities at the location of the wall:

$$u_c^i(x) = u_c^i(u_c(x))$$
$$v_c^i(x) = v_c^i(u_c(x))$$

The simpliest algorithm is the direct method based on Cauchy's integral formula [7]. But other methods may be applied either.

3. Calculation of the model-induced flow field at the location of the wall:

$$u^m(x) = u_c(x) - u_c^i(x)$$
$$v^m(x) = \quad - v_c^i(x)$$

Above equations are valid as far as the small perturbation theory is applicable. The measured flow field is the superposition of the model-induced and the wall-induced flow field.

4. Measurement of the wall pressure distribution with open slots (any position):

$$u_s(x) = -\frac{(c_p)_s}{2}$$
$$v_s(x) = ?$$

Since it is not possible to measure the flow through the slots, no information about the v-component is received.

But it is assumed, that the pressure distribution measured in the centerline of the central slat represents the u-component at the wall. This assumption is supported by the test results of Firmin and Cook [10].

5. Calculation of the wall-induced velocity with open slots:

$$u_s^i(x) = u_s(x) - u^m(x)$$
$$v_s^i(x) = ?$$

This conversion is based on the assumption, that the opening of the slots affects only the wall-induced interference flow field, while the model-induced flow field remains unchanged approximately.

6. Calculation of the v-component of the wall-induced interference flow field from the u-component:

$$v_s^i(x) = v_s^i\left(u_s^i(x)\right)$$

The wall-induced flow field can be represented by a singularity distribution at the location of the wall. Consequently the v^i-distribution is positive defined by the u^i-distribution (see chapter 4).

7. Calculation of the v-component of the homogeneous boundary condition:

$$v_s(x) = v^m(x) + v_s^i(x)$$

From the superposition of the wall-induced and the model-induced v-component the effective v-component of the velocity at the wall with open slots is derived.

8. Calculation of the effective wall shape:

$$\Delta H(x) = \int_{\xi = x_i}^{\xi = x} v_s(\xi) d\xi \qquad (1)$$

The integration of the v-component of the homogeneous wall velocity leads to the effective wall shape.

The effective wall shape is defined as that homogeneous boundary condition, which exerts the same influence on the flow field around the model as the real flow in the slotted test section. This real flow is non-homogeneous because it follows partly the straight slats and interacts partly with the plenum chamber across the slots.

The presented "Two-Step-Method" therefore offers the opportunity to define a homogeneous flow field giving the same effect as the complicated flow field in the vicinity of a slotted test section wall. The procedure requires only standard wall distribution measurements and no model representation.

4. Calculation of the v-component at the wall

The flow field in the test section of a wind tunnel is composed of two parts:

- the model-induced part (flow field around the model in an unlimited domain).
- the wall-induced part
  (influence of the walls to the above mentioned flow field).

Within the small perturbation theory the measured flow field is the linear superposition of both parts.

The model-induced part can be represented by singularities only within the test section. The wall-induced part can be represented either by singularities at the location of the wall or by singularities outside of the wall.

The following procedure becomes simple, if the wall-induced flow field is represented by a vortex distribution in the wall only **(Figure 2)**.

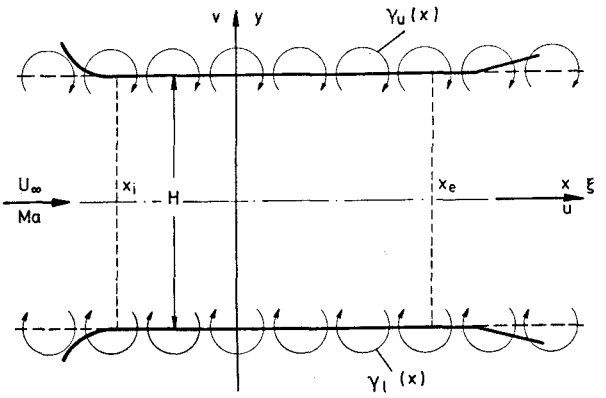

Figure 2. Vortex model

First the u-component induced by the vortex distribution in an arbitrary point of the upper wall is considered. Therefore the induced velocity components of both walls will be integrated. The vortex distribution of the upper wall does not submit any contribution except the vortex in the considered point [11].

Following result is obtained:

$$\beta^2 \cdot U_\infty \cdot \left[1 + u_u^i(x)\right] = -\frac{1}{2} \cdot \gamma_u(x) + \frac{1}{2 \cdot \pi} \int_{-\infty}^{+\infty} \frac{\beta \cdot H}{\beta^2 \cdot H^2 + (\xi - x)^2} \cdot \gamma_l(\xi) \cdot d\xi \tag{2}$$

Accordingly we obtain for an arbitrary point in the lower wall:

$$\beta^2 \cdot U_\infty \cdot \left[1 + u_l^i(x)\right] = +\frac{1}{2} \cdot \gamma_l(x) - \frac{1}{2 \cdot \pi} \int_{-\infty}^{+\infty} \frac{\beta \cdot H}{\beta^2 \cdot H^2 + (\xi - x)^2} \cdot \gamma_u(\xi) \cdot d\xi \tag{3}$$

The compressibility of the fluid is regarded by distortion of the flow field according to "Göthert's rule" [12] with the "Prandtl factor" defined as:

$$\beta = \sqrt{1 - Ma_\infty^2}\,. \tag{4}$$

The analysis is based on an infinite long test section. Upstream and downstream of the region affected by the flow around the model the vortex distribution is constant. This constant part may not be neglected in the integrals (eqs. 2 and 3).

Consequently the integrals are divided into following parts:

$$\begin{aligned} 1 + u_u^i = &-\frac{1}{2 \cdot \beta^2 \cdot U_\infty} \cdot \gamma_u(x) \\ &+ \frac{1}{2 \cdot \pi \cdot \beta^2 \cdot U_\infty} \cdot \int_{x_i}^{x_e} \frac{\beta \cdot H}{\beta^2 \cdot H^2 + (\xi - x)^2} \cdot \gamma_l(\xi) \cdot d\xi \\ &+ \frac{1}{2 \cdot \pi \cdot \beta^2 \cdot U_\infty} \cdot \gamma_l(x_i) \cdot \int_{-\infty}^{x_i} \frac{\beta \cdot H}{\beta^2 \cdot H^2 + (\xi - x)^2} \cdot d\xi \\ &+ \frac{1}{2 \cdot \pi \cdot \beta^2 \cdot U_\infty} \cdot \gamma_l(x_e) \cdot \int_{x_e}^{+\infty} \frac{\beta \cdot H}{\beta^2 \cdot H^2 + (\xi - x)^2} \cdot d\xi \end{aligned} \tag{5}$$

$$\begin{aligned} 1 + u_l^i = &+\frac{1}{2 \cdot \beta^2 \cdot U_\infty} \cdot \gamma_l(x) \\ &- \frac{1}{2 \cdot \pi \cdot \beta^2 \cdot U_\infty} \cdot \int_{x_i}^{x_e} \frac{\beta \cdot H}{\beta^2 \cdot H^2 + (\xi - x)^2} \cdot \gamma_u(\xi) \cdot d\xi \\ &- \frac{1}{2 \cdot \pi \cdot \beta^2 \cdot U_\infty} \cdot \gamma_u(x_i) \cdot \int_{-\infty}^{x_i} \frac{\beta \cdot H}{\beta^2 \cdot H^2 + (\xi - x)^2} \cdot d\xi \\ &- \frac{1}{2 \cdot \pi \cdot \beta^2 \cdot U_\infty} \cdot \gamma_u(x_e) \cdot \int_{x_e}^{+\infty} \frac{\beta \cdot H}{\beta^2 \cdot H^2 + (\xi - x)^2} \cdot d\xi \end{aligned} \tag{6}$$

In the regions, which continue the test section upstream and downstream, the perturbation velocity can be estimated. Therefore the vortex distribution in these terms must be replaced by the perturbation velocity.

With

$$1 + u_i = \frac{\gamma_l(x_i)}{\beta^2 \cdot U_\infty} = -\frac{\gamma_u(x_i)}{\beta^2 \cdot U_\infty} \tag{7}$$

$$1 + u_e = \frac{\gamma_l(x_e)}{\beta^2 \cdot U_\infty} = -\frac{\gamma_u(x_e)}{\beta^2 \cdot U_\infty} \tag{8}$$

we receive the induced perturbation velocity in an arbitrary point of the upper wall:

$$\begin{aligned} 1 + u_u^i = &-\frac{1}{2 \cdot \beta^2 \cdot U_\infty} \cdot \gamma_u(x) \\ &+ \frac{1}{2 \cdot \pi \cdot \beta^2 \cdot U_\infty} \cdot \int_{x_i}^{x_e} \frac{\beta \cdot H}{\beta^2 \cdot H^2 + (\xi - x)^2} \cdot \gamma_l(\xi) \cdot d\xi \\ &+ \frac{1 + u_i}{2 \cdot \pi} \cdot \left(\frac{\pi}{2} + \arctan \frac{x_i - x}{\beta \cdot H} \right) \\ &+ \frac{1 + u_e}{2 \cdot \pi} \cdot \left(\frac{\pi}{2} - \arctan \frac{x_e - x}{\beta \cdot H} \right) \end{aligned} \tag{9}$$

Analogous we receive for an arbitrary point of the lower wall:

$$1 + u_l^l = + \frac{1}{2 \cdot \beta^2 \cdot U_\infty} \cdot \gamma_l(x) - \frac{1}{2 \cdot \pi \cdot \beta^2 \cdot U_\infty} \cdot \int_{x_i}^{x_e} \frac{\beta \cdot H}{\beta^2 \cdot H^2 + (\xi - x)^2} \cdot \gamma_u(\xi) \cdot d\xi + \frac{1 + u_i}{2 \cdot \pi} \cdot \left(\frac{\pi}{2} + \arctan \frac{x_i - x}{\beta \cdot H} \right) + \frac{1 + u_e}{2 \cdot \pi} \cdot \left(\frac{\pi}{2} - \arctan \frac{x_e - x}{\beta \cdot H} \right) \quad (10)$$

Depending on the height of the test section the first term of the right hand side of equation 9 resp. equation 10 dominates more or less. Therefore an iterative solution for the calculation of the vortex distribution is advantageous with following first step:

$$\frac{\gamma_l(x)}{\beta^2 \cdot U_\infty} = 1 + u_l^i \quad (11)$$

The iteration converges fast and in all test cases the final value was reached after few steps.

From the calculated vortex distribution the v-component of the wall-induced velocity can be calculated. For the upper wall it is obtained [11]:

$$\beta \cdot U_\infty \cdot v_u^i(x) = \frac{1}{2 \cdot \pi} \cdot \int_{-\infty}^{+\infty} \frac{1}{\xi - x} \cdot \gamma_u(\xi) \cdot d\xi + \frac{1}{2 \cdot \pi} \cdot \int_{-\infty}^{+\infty} \frac{\xi - x}{\beta^2 \cdot H^2 + (\xi - x)^2} \cdot \gamma_l(\xi) \cdot d\xi \quad (12)$$

Analogous for the lower wall:

$$\beta \cdot U_\infty \cdot v_l^i(x) = \frac{1}{2 \cdot \pi} \cdot \int_{-\infty}^{+\infty} \frac{1}{\xi - x} \cdot \gamma_l(\xi) \cdot d\xi + \frac{1}{2 \cdot \pi} \cdot \int_{-\infty}^{+\infty} \frac{\xi - x}{\beta^2 \cdot H^2 + (\xi - x)^2} \cdot \gamma_u(\xi) \cdot d\xi \quad (13)$$

Because of the constant vortex distribution upstream and downstream of the test section (see eq 7 and 8) it holds for the upper wall:

$$v_u^l(x) = \frac{1}{2 \cdot \pi \cdot \beta \cdot U_\infty} \cdot \int_{x_i}^{x_e} \frac{1}{\xi - x} \cdot \gamma_u(\xi) \cdot d\xi + \frac{1}{2 \cdot \pi \cdot \beta \cdot U_\infty} \cdot \int_{x_i}^{x_e} \frac{\xi - x}{\beta^2 \cdot H^2 + (\xi - x)^2} \cdot \gamma_l(\xi) \cdot d\xi + \frac{\beta}{4 \cdot \pi} \cdot (1 + u_i) \cdot \ln \left[1 + \left(\frac{\beta \cdot H}{x_i - x} \right)^2 \right] - \frac{\beta}{4 \cdot \pi} \cdot (1 + u_e) \cdot \ln \left[1 + \left(\frac{\beta \cdot H}{x_e - x} \right)^2 \right] \quad (14)$$

Analogous for the lower wall:

$$v_l^l(x) = \frac{1}{2 \cdot \pi \cdot \beta \cdot U_\infty} \cdot \int_{x_i}^{x_e} \frac{1}{\xi - x} \cdot \gamma_l(\xi) \cdot d\xi + \frac{1}{2 \cdot \pi \cdot \beta \cdot U_\infty} \cdot \int_{x_i}^{x_e} \frac{\xi - x}{\beta^2 \cdot H^2 + (\xi - x)^2} \cdot \gamma_u(\xi) \cdot d\xi - \frac{\beta}{4 \cdot \pi} \cdot (1 + u_i) \cdot \ln \left[1 + \left(\frac{\beta \cdot H}{x_i - x} \right)^2 \right] + \frac{\beta}{4 \cdot \pi} \cdot (1 + u_e) \cdot \ln \left[1 + \left(\frac{\beta \cdot H}{x_e - x} \right)^2 \right] \quad (15)$$

5. Experimental Verification

The first experimental examination of the presented "Two-Step-Method" was conducted in the Transonic Wind Tunnel Braunschweig [13] [14]. The test section of this wind tunnel is designed especially for profile investigations in the sub- and transonic regime. The side walls are closed and the upper and the lower wall are equipped each with 6 longitudinal slots with an open-area ratio of $\sigma = 2{,}35$ %. The slots are fix and therefore the tests could be conducted only with this fixed wall-opening and with closed walls (Slots temporary closed by self-adhesive aluminium tape).

The extensive verification of the "Two-Step-Method" was conducted in the Transonic Wind Tunnel Göttingen with 1m × 1m test section size and variable stagnation pressure. Originally this wind tunnel was equipped with a perforated test section wall (6% open-area ratio, 30° inclined holes). After reconstruction in 1987 the side walls are closed. Top and bottom wall are replaced by 5 longitudinal slats from which the central one is fixed and the outer four are adjustable. These slats are comprising slots with an open-area ratio from zero (closed) to $\sigma = 15$ %. The investigation below refers only to the tests in the Göttingen tunnel.

The wall pressure distribution is measured in the centerline of the middle slat. This is the plane of symmetry of the test section. The lines in the top and the bottom wall comprise 32 pressure taps each.

The local perturbation velocity is calculated from the local pressure by the well-known linearized equation:

$$u = -\frac{c_p}{2} \quad (16)$$

It is assumed that the perturbation velocity vanishes upstream of the test section:

$$u_l = 0 \quad (17)$$

For tests with a model the residual perturbation velocity downstream of the test section may not be neglected. For the actual tests this velocity was estimated from the drag coefficient.

From the momentum equation we receive for the drag:

$$D = H \cdot W \cdot \left[\rho_e \cdot U_\infty^2 \cdot (1 + u_e)^2 - \rho_\infty \cdot U_\infty^2 \right] \quad (18)$$

From the continuity equation we obtain:

$$\rho_\infty \cdot U_\infty = \rho_e \cdot U_\infty \cdot (1 + u_e) \tag{19}$$

The drag coefficient is defined as:

$$c_D = \frac{D}{W \cdot L \cdot \frac{\rho_\infty}{2} \cdot U_\infty^2} \tag{20}$$

Summarizing equations 18, 19, and 20 yields:

$$u_e = \frac{L}{H} \cdot \frac{c_D}{2} \tag{21}$$

This constant velocity is assumed as perturbation velocity downstream of the test section.

The calibration program for the empty test section had to consider the conduction of tests with 2D-models (profile tests) and the conduction of tests with 3D-models in the test section.

For the tests with 2D-models following constellation was established:

- parallel side walls
- suction rate optimized for each slot open-area ratio

For the test with 3D-models following constellation was established:

- no suction
- side wall angle (divergent) optimized for each slot open-area ratio

This calibration procedure was performed for the subsonic and the transonic range. The dependency of the calibration from the Reynolds number was checked, but can be neglected.

6. Tests with the Empty Test Section

The new developed "Two-Step-Method" was first examined by tests in an empty test section. In this special case the real velocity distribution is identical with the wall-induced flow field (wall interferences), because no model-induced flow field is present. If a non-disturbing probe (for example a lance probe) is at disposal, it is possible to check the validity of the above deduced method directly.

For this test a lance probe was mounted in the center-line of the test section. Accordingly the wall-induced flow field has been calculated for this location.

For the compensation of the displacement thickness of the boundary layer, the side walls of the test section were adjusted with 0.5° divergence each (Calibration for 3D-models).

Figure 3 shows in the *lower diagram* the measured velocity distribution in the center-line of the top and the bottom wall for the closed and the slotted (σ = 1%) test section. Although the test section walls are assembled from grinded stainless steel plates, the measured values show some scattering. From these velocity distributions the velocity distribution in the center-line of the test section (defined as wall-interferences) was calculated. The result is shown in the *upper diagram* of **Figure 3** and compared with the values measured with the lance probe. It has to be taken into account, that the perturbations are very small as indicated by the mark for Δp = 0,1%. This is the (optimistic estimated) measuring tolerance. On the other hand it is not evident, that it is permitted to utilize the 2D-formula system in the empty test section without a 2D-model. Under these considerations the agreement between the measured points and the related curves seems to be rather good. **Figure 4** shows a similar test result, but with a slot opening-area ratio of σ = 2%. The comparison of Figure 3 and Figure 4 demonstrates the typical behaviour of the slotted wall (outflow - inflow), but the opening of 1% is a little too small and 2% a little large. Consequently the optimum open-area ratio can be assumed between these values.

7. Evaluation and Presentation of the Profile Tests

For the investigation of wall interferences it is advantageous to apply symmetrical models, because they give the chance to decide between blockage and lift effects. Since larger effects can be expected with larger models, the largest available model, a NACA 0012-profile with 300 mm chord-length was chosen for the validation tests.

The program for the tests with model comprised the pressure distribution in the center-line of top and bottom wall and in the center-plane of the profile.

Following parameters have been varied during the tests:

- slot open-area ratio (σ = 0; 2; 4; 6%)
- Mach number (Ma = 0,6; 0,7; 0,8)
- angle of incidence (α = 0; 2; 5; 10°)

Only few examples from this extensive amount of results can be presented.

Presentation of wall pressure distribution:

The evaluation of the wall pressure distribution for each slot opening is compared with the corresponding test with closed slots. The results are compiled in a group of three diagrams (see for example **Figure 5).**

The *lower diagram* shows the measured perturbation velocity at the wall. The values are interpolated by a spline. Upstream of the test section the values are approximating (eq. 17):

$$u_i = 0; \ (x \to -\infty)$$

Downstream of the test section the values are approximating (eq. 21):

$$u_e = \frac{L}{H} \cdot \frac{c_D}{2}; \ (x \to +\infty)$$

Additional the perturbation velocity at the wall for interference-free flow was calculated and entered into the diagram.

The *middle diagram* shows the corresponding wall deflections. Only the straight closed wall is a real existing wall. The so-called "slotted wall" is the contour of a closed deflected wall with the same influence to the flow field as the slotted one. Analogous indicates "interference-free" the calculated contour of an adapted wall for interference-free flow around the model.

The *upper diagram* shows the calculated wall-induced interference velocities for the closed and the slotted wall. (This verlocity is zero for the adapted wall as defined).

Presentation of the profile pressure distribution:

The evaluation of the profile pressure distribution for each slot configuraton contains the measured and the calculated interference-free distribution (see for example **Figure 6).** For comparison a theoretical calculated pressure distribution from the well-known NACA compilation [15] has been added.

The compressibily effects for the theoretical distribution are calculated by the Prandtl-Glauert-rule.

With symmetrical profiles it is always difficult to show the curves as distinct as necessary. Therefore in the presented diagrams the velocity distribution for the lower side has been turned about.

Figure 5 shows the evaluation of the wall pressure distribution for $\alpha = 0°$ (blockage effect only) and for the lowest investigated Mach number. The residual interferences are lowered by the opening of the slots considerable. This result is supported by the comparison of the wall deflections. The shifting of the slotted wall contour caused by the residual v-component does not affect the profile pressure distribution (Figure 6) and can be neglected in this discussion. Moreover Figure 6 and **Figure 7** demonstrate a good agreement with the theoretical pressure distribution. Only in the region of maximum profile thickness non-linear effects (not coverd by the wall-interference theory) are evident. This effect increases with the Mach number (**Figure 8). Figure 9** (Ma = 0,8) shows the typical pressure distribution of a local supersonic region which is closed by a shock. This situation is far beyond the application range of the "Two-Step-Method" as presented in this paper.

The evaluation of the wall pressure distribution for a model with lift (and blockage) is shown in **Figure 10** . From the residual interferences it can be concluded that the u-component has been lowered substantially, but the v-component increases a little. This may be compensated by different slot openings in the top and the bottom wall. But for a slender body and small angles of attack the v-correction may be neglected (**Figure 11** and **Figure 12**).

8. Application of the Two-Step-Method

With the Two-Step-Method we are capable to calculate the residual wall interferences and the effective wall deflection from two corresponding tests for a defined slot position. This procedure is not reversible. Therefore it is not possible to calculate the slot open-area ratio required for zero or at least minimal residual interferences and more than one test may be necessary for the definition of the optimum slot position. Consequently an appropriate procedure has to be outlined to minimize the effort for optimizing the slot position.

In general a complete compensation of the wall interferences requires a variable slot parameter as function of x for the top and the bottom wall (tailored slots). The slotted walls of the Transonic Wind tunnel Göttingen are designed for different slot positions in the top and the bottom wall and up- and downstream of the test section (tapered slots). But the recent test program was conducted with one control value only (all slot positions equal).

The constant part of the residual interferences can be considered by a correction of the Mach number ($u' = const$) or the angle of incidence ($v' = const$), i.e. a superpositon of a homogeneous flow field. But the non-constant parts of the residual interferences (acceleration or curvature of the flow) can only be compensated approximately. Therefore the open-area ratio of the slot should primarily defined with respect to minimize the non-constant parts of the residual interferences.

The "Two-Step-Method" requires one test with closed walls. Therefore it failes at higher Mach numbers, if the local supersonic flow field of the model reaches the wall and the flow chokes.

9. Conclusion

For wind tunnel test sections with adjustable slotted walls and 2D-models a "Two-Step-Method" has been developed for the determination of the residual interferences and the effective contour of an virtual adaptive wall.

The method is based on two corresponding tests, one with closed and one with open slots, and all other conditions unchanged. No model representation is required.

The method is restricted to moderate Mach numbers with at least non-choking flow conditions during the closed-wall test.

The method has been checked successfull in an empty test section by comparison with lance probe measurements. Systematic tests have conducted with the symmetrical profile NACA 0012.

10. Bibliography

[1] Göthert, B.
Transonic Wind Tunnel Testing
AGARD Rep. 49, Pergamon Press 1961

[2] Guderley, G.
Simplifications of the Boundary Conditions at a Wind-Tunnel Wall with Longitudinal Slots
WADC Rep. 53-150 (1953)

[3] Baldwin, Jr.,B.S.; Turner, J.G.; Knechtel, E.D.
Wall Interference in Wind Tunnels with Slotted and with Slotted and Porous Boundaries at Subsonic Speeds
NACA TN 3176 (1954)

[4] Davis, D.D.; Moore, D.
Analytical Studies of Blockage- and Lift-Interference Corrections for Slotted Tunnels Obtained by the Substitution of an Equivalent Homogeneous Boundary for the Discrete Slots
NACA RM-L 53 E 07b (1953)

[5] Maeder, P.F.
Theoretical Investigation of Subsonic Wall Interference in Rectangular Slotted Test Sections
Brown University, Division of Eng., Techn. Rep. WT-11 (1953)

[6] Berndt, S.B.; Sörensen, H.
Flow Properties of Slotted Walls for Transonic Test Sections
AGARD-CP-174 (1976) S. 17.1 - 17.10

[7] Amecke, J.
Direkte Berechnung von Wandinterferenzen und Wandadaption bei zweidimensionaler Strömung in Windkanälen mit geschlossenen Wänden
DFVLR-FB 85-62 (1985)

[8] Parker,Jr.R.L.; Erickson,Jr.,J.C.
Development of a Three-Dimensional Adaptive Wall Test Section with Perforated Walls
AGARD-CP-335 (1982), S. 17.1 - 17.14

[9] Schairer, E.T.
Two-Dimensional Wind-Tunnel Interference from Measurements on Two-Contours
J. Aircraft 21 (1984), S. 414-419

[10] Firmin, M.C.P.; Cook, P.H.
Disturbances from Ventilated Tunnel Walls in Aerofoil Testing
AGARD-CP-348 (1984), S. 8.1 - 8.15

[11] Schlichting, H.; Truckenbrodt, E.
Aerodynamik des Flugzeuges
Berlin, Göttingen, Heidelberg: Springer Verlag 1959

[12] Göthert, B.
Ebene und räumliche Strömung bei hohen Unterschallgeschwindigkeiten
Jahrb. dt. Lufo 1941, S. I 156-158

[13] Stanewsky, E.; Puffert-Meissner, W.; Müller, R.; Hoheisel, H.
Der Transsonische Windkanal Braunschweig der DFVLR
Z. Flugwiss. 6 (1982), S. 328-408

[14] Amecke, J.
Zweischrittmethode zur Bestimmung der zweidimensionalen Wandinterferenzen in geschlitzten Windkanalwänden
DLR Report IB 222 - 85 A 32 (1986)

[15] Abbott, I.H.; Doenhoff, A.E. von; Stivers jr., L.S.
Summary of Airfoil Data
NACA Report No. 824 (1945)

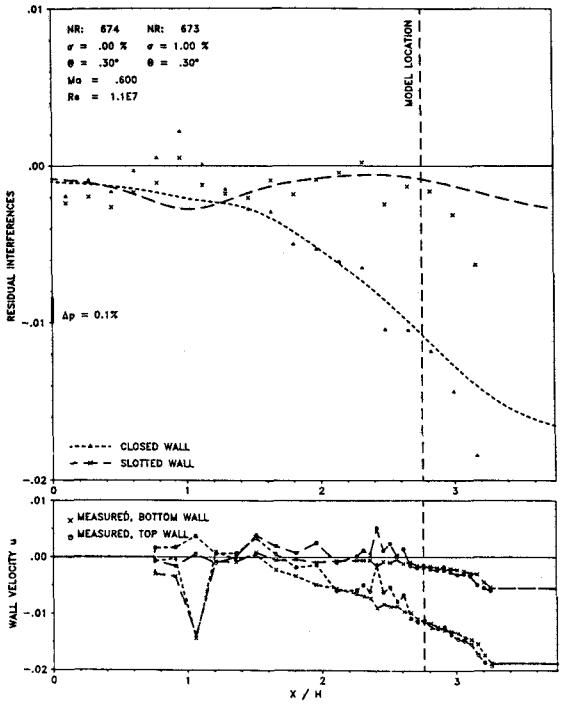

Figure 3. Velocity distribution in an empty test section
σ = 0 % and 1 %

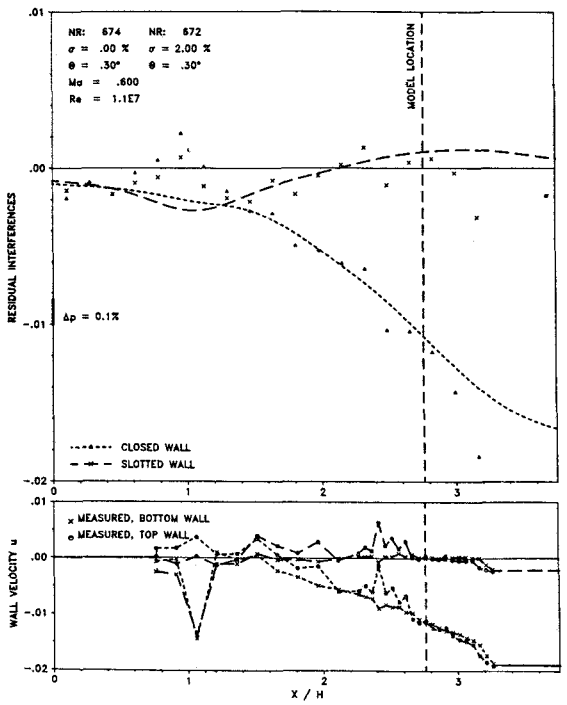

Figure 4. Velocity distribution in an empty test section
σ = 0 % and 2 %

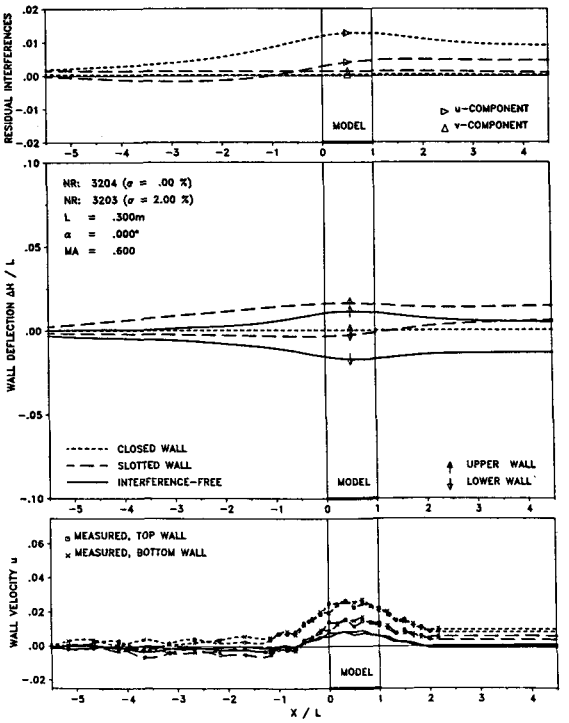

Figure 5. Wall velocity and deflection distribution
$Ma_\infty = 0{,}6$; $\alpha = 0°$; $\sigma = 0$ and 2%

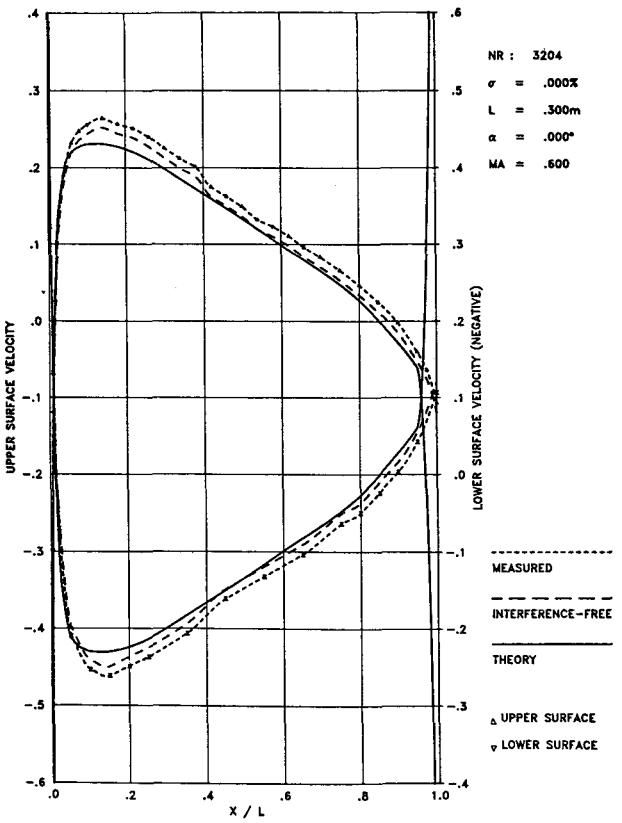

Figure 6. Profile surface pressure distribution
$Ma_\infty = 0{,}6$; $\alpha = 0°$; $\sigma = 0\%$

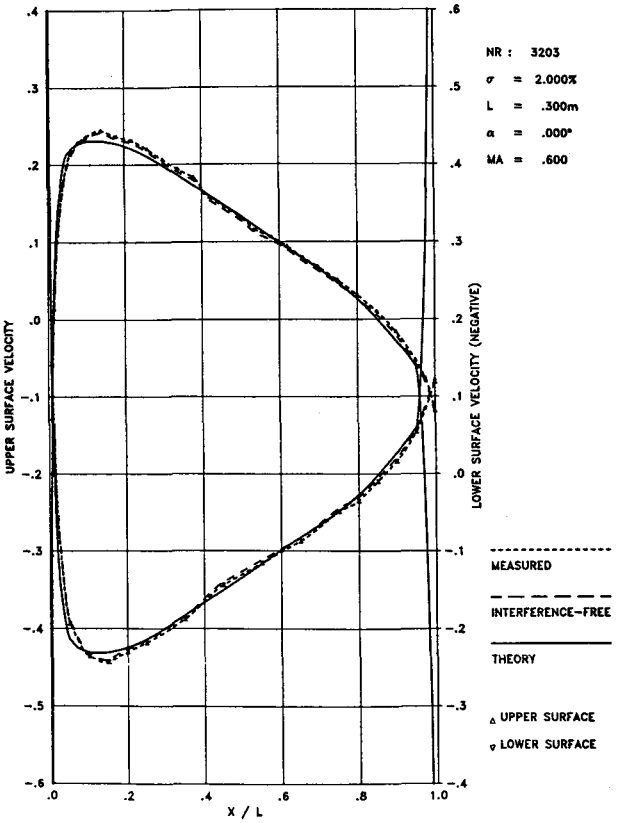

Figure 7. Profile surface pressure distribution
$Ma_\infty = 0{,}6$; $\alpha = 0°$; $\sigma = 2\%$

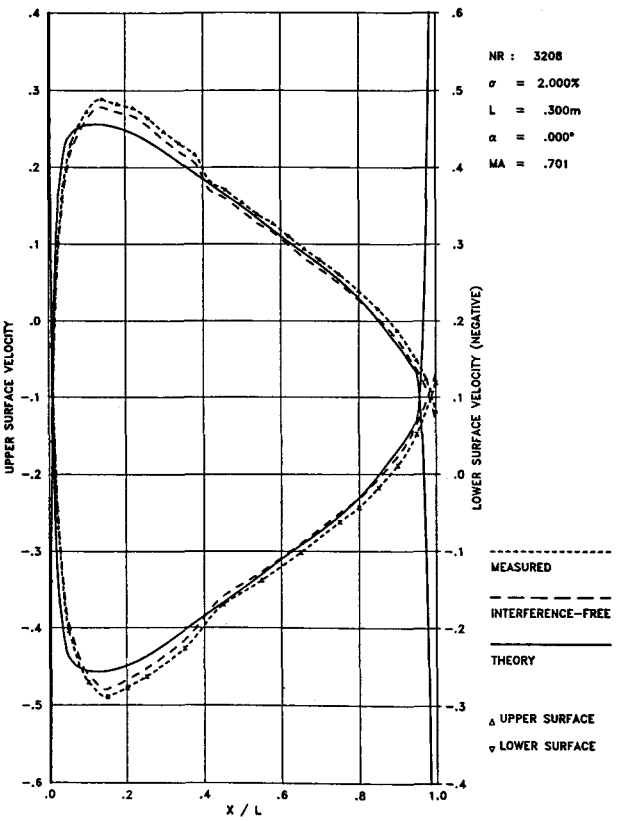

Figure 8. Profile surface pressure distribution
$Ma_\infty = 0{,}7$; $\alpha = 0°$; $\sigma = 2\%$

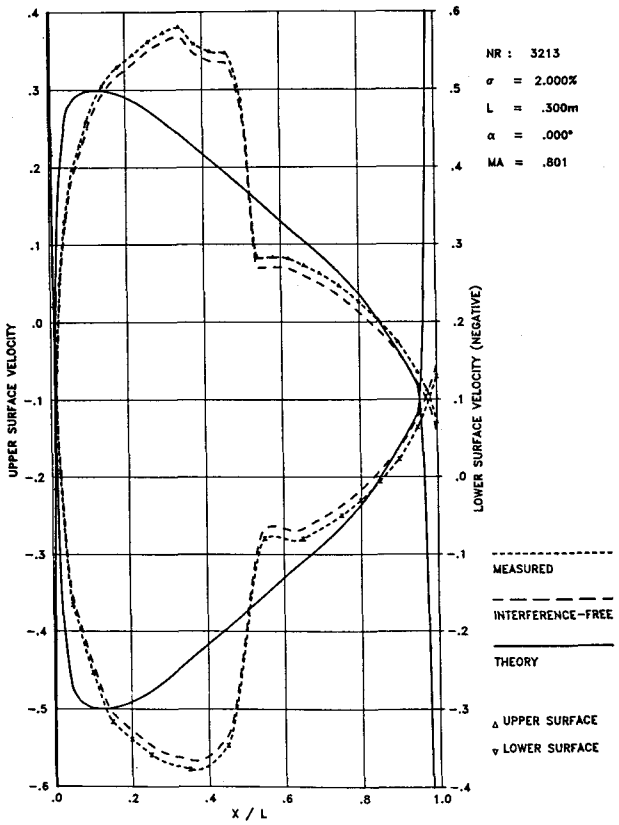

Figure 9. **Profile surface pressure distribution**
$Ma_\infty = 0{,}8$; $\alpha = 0°$; $\sigma = 2\%$

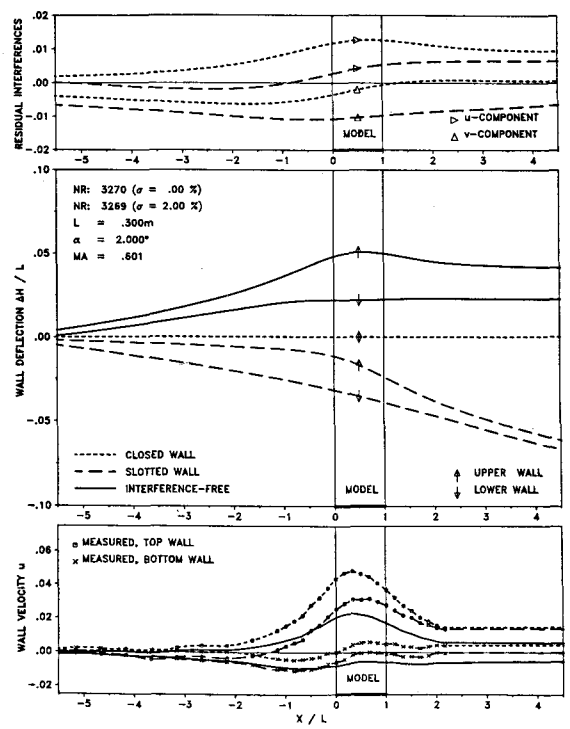

Figure 10. **Wall velocity and deflection distribution**
$Ma_\infty = 0{,}6$; $\alpha = 2°$; $\sigma = 0$ and 2%

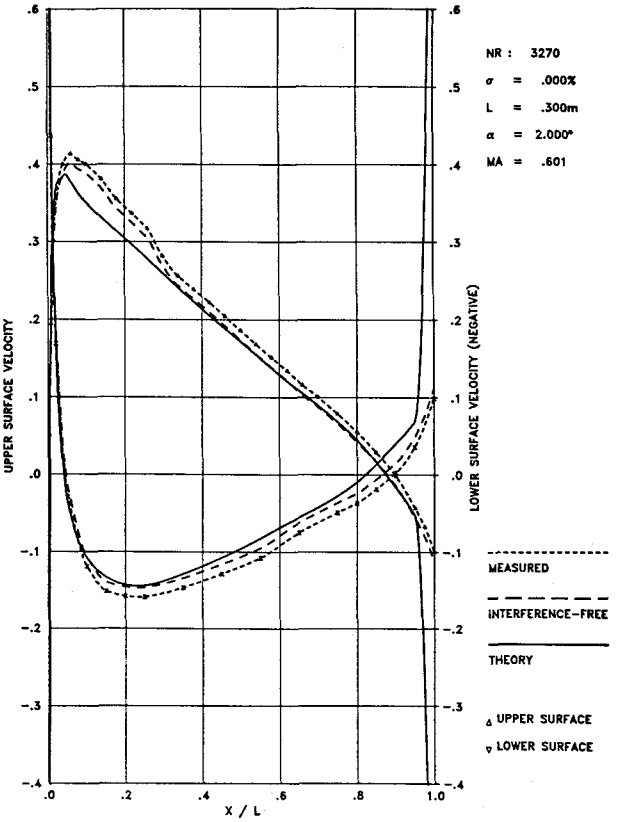

Figure 11. **Profile surface pressure distribution**
$Ma_\infty = 0{,}6$; $\alpha = 2°$; $\sigma = 0\%$

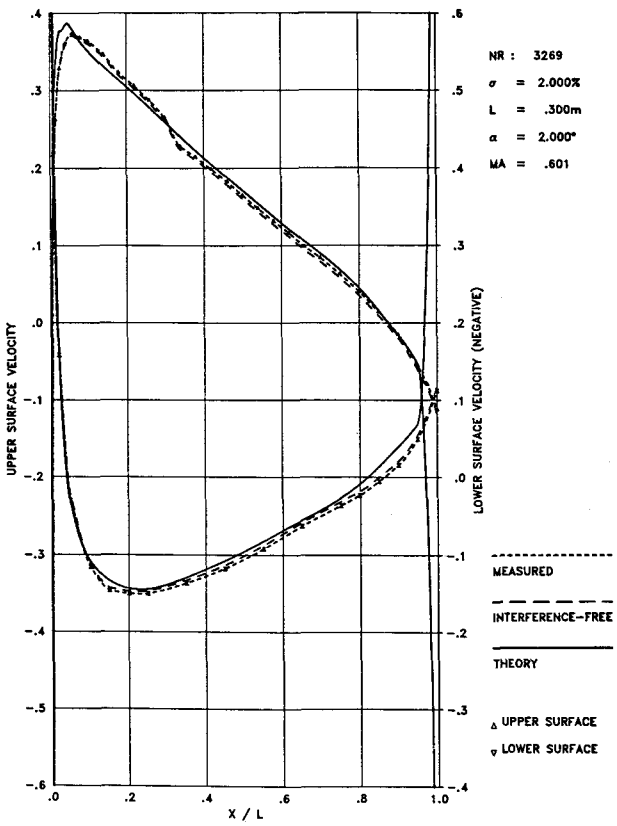

Figure 12. **Profile surface pressure distribution**
$Ma_\infty = 0{,}6$; $\alpha = 2°$; $\sigma = 2\%$